Int. J. Heat Mass Transfer. Vol. 29, No. 2, pp. 309–315, 1986
Printed in Great Britain

0017–9310/86 $3.00 + 0.00
Pergamon Press Ltd.

Free boundary shape of a convectively cooled solidified region

ROBERT SIEGEL
Lewis Research Center, Cleveland, OH 44135, U.S.A.

(*Received* 11 *June* 1985 *and in final form* 12 *September* 1985)

Abstract—The two-dimensional steady-state shape of a solidified region, such as a frost layer, was determined analytically for formation on a plate that is convectively cooled. The nonuniform shape of the layer is produced by exposure to a spatially nonuniform distribution of radiant energy. For high convective cooling the cooled wall approaches a uniform temperature, and an exact solution is obtained for the free boundary shape. For a lesser amount of convective cooling, the variation in temperature along the cooled boundary is treated by a boundary perturbation method. Some illustrative examples are given that show the effects of nonuniform heating and the magnitude of convective heat transfer at the cooled wall. Only one boundary condition is approximated by the perturbation solution; all of the other boundary conditions are satisfied exactly. The calculated results given here were found to satisfy the approximate boundary condition within a very small error.

INTRODUCTION

AN INTERESTING class of problems are those involving unknown, or 'free' boundaries. Steady-state and moving free boundaries have been studied in connection with solidification and melting processes [1], flows in porous media [2], design of tool shapes for electrochemical machining [3], prediction of shapes of jets and bubbles [4], as well as many other types of inverse problems. In the last decade there has been an increased effort toward the development of numerical inverse methods. An example is in ref. [5] where a numerical solution was obtained for a steady-state free boundary solidification problem that had been solved analytically in ref. [6]. Since the presence of an unknown boundary usually provides difficulties in both numerical and analytical methods, advances in either of these approaches, or in their combination, are welcome additions to the development of this area. Analytical solutions provide a very helpful insight into free boundary behavior and provide a comparison for numerical results.

In the present work a few mathematical ideas will be combined to obtain the steady response of a solidified layer to imposed, spatially variable, radiative heating along one face. The other side of the layer is being cooled by convection, and thus the temperature distribution along this boundary is unknown and will be determined in conjunction with finding the free boundary shape. The analytical procedure involves inverting the problem so that the physical coordinates are to be found as dependent variables of the temperature and a heat flow function orthogonal to the constant temperature lines. This transformation maps the solidified region into a region that is approximately rectangular; if the cooled wall were at uniform temperature the region would be a rectangle. A boundary perturbation method [7] was applied to transfer the conditions to a fully rectangular shape, and an analytical solution was then obtained.

The physical system is most easily described by referring to Fig. 1(a). The solidified region could be a frost layer formed on a cooled surface in the presence of incident radiation, or a layer could be machined by application of radiative energy. Another interpretation would be finding the shape of a layer that is to be controlled at a uniform surface temperature while exposed to nonuniform heating and being convectively cooled at the other surface. A particular problem of this type was solved by conformal mapping in ref. [8].

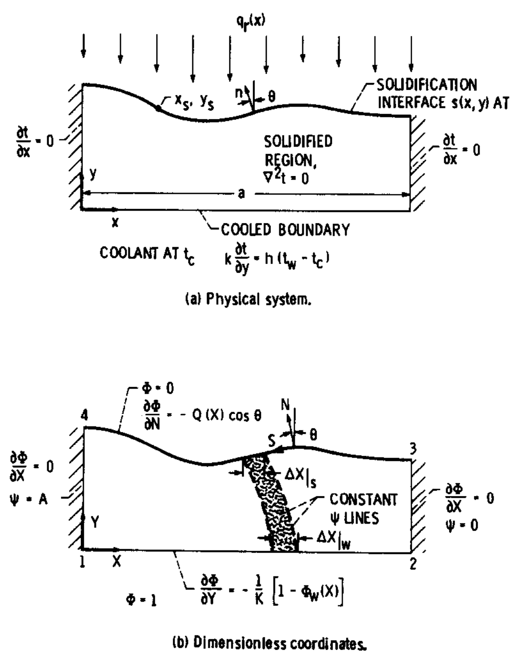

FIG. 1. Solidified region on convectively cooled boundary.

NOMENCLATURE

A dimensionless length and dimensionless parameter, $(\alpha q_{r,m} a)/[k(t_f - t_c)] = a/y_m$
a width of solidified region
C_n, E_n coefficients in Fourier series solution
h convective heat transfer coefficient at cooled boundary
K dimensionless parameter, k/hy_m
k thermal conductivity of solidified material
n normal to solidification interface, $N = n/y_m$
Q dimensionless heat flux, $q_r/q_{r,m}$
q_r incident radiant heat flux; $q_{r,m}$, integrated mean value of q_r
S dimensionless coordinate along solidification interface
t temperature
X_0, X_I zeroth- and first-order terms in expansion of $X(\Psi, \Phi)$
x, y coordinates in physical plane; $X = x/y_m$, $Y = y/y_m$
Y_0, Y_I zeroth- and first-order terms in expansion of $Y(\Psi, \Phi)$
y_m thickness, $k(t_f - t_c)/\alpha q_{r,m}$.

Greek symbols
α radiant absorptivity of surface
θ angle between interface normal and y-axis
Φ potential function, $(t_f - t)/(t_f - t_c)$
Ψ heat flow function orthogonal to Φ

Subscripts
c at coolant temperature
f at solidification temperature
m mean value
r radiant
s at solidification interface
w at cooled wall of layer.

ANALYSIS

Problem description

The solidified region is shown in Fig. 1(a). It has a shape that depends upon an incident distribution of radiant energy that varies along the x-direction. The absorbed energy is conducted through the solidified region and removed from the cooled boundary by convection with a constant heat transfer coefficient to a coolant at t_c. The side walls can be either insulated or represent symmetry planes for a periodic variation of $q_r(x)$. These conditions provide the following boundary conditions. At the side boundaries,

$$\frac{\partial t}{\partial x} = 0 \quad x = 0, a \quad y > 0. \tag{1}$$

At the solidification interface,

$$t = t_f \tag{2}$$

$$k\frac{\partial t}{\partial n} = \alpha q_r(x) \cos\theta. \tag{3}$$

At the cooled boundary,

$$k\frac{\partial t}{\partial y} = h[t_w(x) - t_c]. \tag{4}$$

Within the solidified region the heat conduction equation applies

$$\frac{\partial^2 t}{\partial x^2} + \frac{\partial^2 t}{\partial y^2} = 0. \tag{5}$$

It is noted that the boundary conditions are overspecified in the sense that equations (2) and (3) provide both the temperature and its normal derivative along one boundary. It is the shape of the solidification interface that is unknown. The convective condition, equation (4), contains the wall temperature distribution which is also an unknown and will be determined during the analytical solution that follows.

To place the equations in dimensionless form, a mean incident heat flux is defined as

$$q_{r,m} = \frac{1}{a}\int_0^a q_r(x)\,dx. \tag{6}$$

If the incident heating is uniform at $q_{r,m}$ the solidified layer will have a uniform thickness. When the convection coefficient $h \to \infty$ then $t_w \to t_c$ and this layer thickness is

$$y_m = \frac{k(t_f - t_c)}{\alpha q_{r,m}}. \tag{7}$$

This will be used as a reference dimension in what follows.

Region in potential plane

The analysis is carried out by mapping the solidified region into a potential plane. First the region is placed in dimensionless form as shown in Fig. 1(b). A temperature potential function is defined by the ratio $\Phi = (t_f - t)/(t_f - t_c)$; since $t_c \leqslant t \leqslant t_f$, then $0 \leqslant \Phi \leqslant 1$. Then using the quantities defined in the Nomenclature, equation (1) becomes along the side walls

$$\frac{\partial \Phi}{\partial X} = 0 \quad X = 0, A \quad Y > 0. \tag{8}$$

Equations (2) and (3) are

$$\Phi = 0 \tag{9}$$

$$-\frac{\partial \Phi}{\partial N} = Q(X)\cos\theta. \tag{10}$$

At the convectively cooled wall

$$-\left.\frac{\partial \Phi}{\partial Y}\right|_w = \frac{1}{K}[1-\Phi_w(X)]. \tag{11}$$

The heat conduction equation becomes

$$\frac{\partial^2 \Phi}{\partial X^2} + \frac{\partial^2 \Phi}{\partial Y^2} = 0. \tag{12}$$

Since heat flow is normal to constant temperature lines, a heat flow function Ψ can be defined, where lines of constant Ψ and Φ form an orthogonal grid. Each pair of Ψ lines bounds a fixed amount of heat flow. Now consider a potential plane as shown in Fig. 2. Since $\Phi = 0$ along the solidification boundary, the boundary $\widehat{34}$ is along the Ψ-axis. Along the cooled wall the Φ is an unknown variable that will be between 0 and 1; hence the curve $\widehat{12}$ has an unknown shape. When $h \to \infty$ the cooled wall will be at t_c which gives the upper limit dashed boundary along which $\Phi_w = 1$. The boundaries $\widehat{14}$ and $\widehat{23}$ have no heat crossing them; hence they are along constant heat flow lines.

The analysis will now proceed by letting X, Y be dependent variables of Ψ, Φ. Since Ψ, Φ are analytic functions of X, Y, then X, Y are conjugate harmonic functions of Ψ, Φ and satisfy,

$$\frac{\partial^2 \xi}{\partial \Psi^2} + \frac{\partial^2 \xi}{\partial \Phi^2} = 0, \quad \text{where} \quad \xi = X \quad \text{or} \quad Y. \tag{13}$$

To solve these equations the boundary conditions for X and/or Y are needed for the region in Fig. 2. Along $\widehat{14}$, $X = 0$ and along $\widehat{23}$, $X = A$. On the interface $\widehat{34}$,

$$\left.\frac{\partial \Psi}{\partial X}\right|_s = \left(\frac{\partial \Psi}{\partial S}\frac{\partial S}{\partial X} + \frac{\partial \Psi}{\partial N}\frac{\partial N}{\partial X}\right)_s. \tag{14}$$

Then along $\widehat{34}$, which is at constant temperature, the Cauchy–Rieman equations give $\partial\Phi/\partial N = -\partial\Psi/\partial S$ and $\partial\Psi/\partial N = \partial\Phi/\partial S = 0$. It follows that with $\partial S/\partial X = -1/\cos\theta$, and by use of equation (10),

$$\left.\frac{\partial \Psi}{\partial X}\right|_s = -Q(X). \tag{15}$$

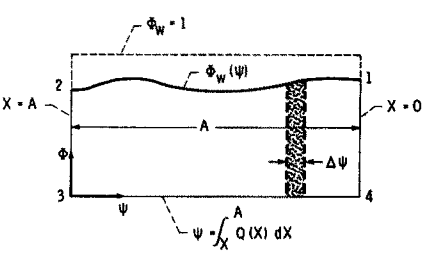

FIG. 2. Region in potential plane.

Letting $\Psi = 0$ at $X = A$, this integrates to give along $\widehat{34}$,

$$\Psi(X) = \int_X^A Q(X)\,dX. \tag{16}$$

Then by use of equation (6) placed in dimensionless form, the maximum Ψ is

$$\Psi_{max} = \int_0^A Q(X)\,dX = A. \tag{17}$$

Thus the width of the region in Fig. 2 is A. Equation (16) provides the boundary condition between X and Ψ along $\widehat{34}$.

Next the boundary condition will be considered along the cooled boundary $\widehat{12}$. A heat flow channel between two almost equal Ψ lines is shown shaded in Fig. 1(b). A heat balance on this channel gives

$$\alpha q_r(x)\Delta X|_s = h\Delta X|_w[t_w(x) - t_c].$$

Equation (15) is used on the LHS and the result is placed in dimensionless form to obtain (note from the shaded region mapped into Fig. 2 that $\Delta\Psi|_s = \Delta\Psi|_w$),

$$-K\Delta\Psi|_s = -K\Delta\Psi|_w = \Delta X|_w[1-\Phi_w(X)]. \tag{18}$$

Along the cooled wall the X is a function of both Ψ and Φ so that

$$\left.dX\right|_w = \left(\left.\frac{\partial X}{\partial \Psi}\right|_\Phi d\Psi + \left.\frac{\partial X}{\partial \Phi}\right|_\Psi d\Phi\right)_w. \tag{19}$$

Also along the wall, Y is zero so that

$$\left(\left.\frac{\partial Y}{\partial \Psi}\right|_\Phi d\Psi + \left.\frac{\partial Y}{\partial \Phi}\right|_\Psi d\Phi\right)_w = 0.$$

Applying the Cauchy–Riemann conditions yields along w,

$$\left.\frac{\partial X}{\partial \Phi}\right|_\Psi = \left.\frac{\partial X}{\partial \Psi}\right|_\Phi \frac{d\Phi}{d\Psi}.$$

This is substituted into equation (19) to obtain

$$\left.\frac{dX}{d\Psi}\right|_w = \left\{\left.\frac{\partial X}{\partial \Psi}\right|_\Phi \left[\left(\frac{d\Phi}{d\Psi}\right)^2 + 1\right]\right\}_w.$$

Then the boundary condition equation (18) becomes

$$-K = \left\{\left.\frac{\partial X}{\partial \Psi}\right|_\Phi \left[\left(\frac{\partial \Phi}{\partial \Psi}\right)^2 + 1\right]\right\}_w [1-\Phi_w(X)]. \tag{20}$$

Perturbation analysis

The curved upper boundary $\widehat{12}$ in the potential plane in Fig. 2 has an unknown shape. When $h \to \infty$ this curve becomes the upper dashed straight line, and the solidified region is then a rectangle in the potential plane. A boundary perturbation method will now be used to transfer conditions from $\widehat{12}$ to the upper dashed line. Then an analytical solution can be obtained by solving in the rectangular region. The quantity $K = k/hy_m$ will be used as the perturbation parameter, so the solution is being perturbed from the analytical solution that will be obtained for $h \to \infty$. The

$X(\Psi, \Phi)$ and $Y(\Psi, \Phi)$ are expanded into the forms

$$X(\Psi, \Phi) = X_0(\Psi, \Phi) + KX_{\rm I}(\Psi, \Phi) + K^2X_{\rm II}(\Psi, \Phi) + \cdots \quad (21a)$$

$$Y(\Psi, \Phi) = Y_0(\Psi, \Phi) + KY_{\rm I}(\Psi, \Phi) + K^2X_{\rm II}(\Psi, \Phi) + \cdots. \quad (21b)$$

The X and Y along the upper dashed line ($\Phi = 1$) in Fig. 2 can also be expressed by a Taylor series expansion upward from the $\widehat{12}$ boundary. Then after using equations (21a) and (21b)

$$X_0(\Psi, 1) + KX_{\rm I}(\Psi, 1) + \cdots = X(\Psi, \Phi_w) + (1-\Phi_w)\left.\frac{\partial X}{\partial \Phi}\right|_w + \cdots \quad (22a)$$

$$Y_0(\Psi, 1) + KY_{\rm I}(\Psi, 1) + \cdots = Y(\Psi, \Phi_w) + (1-\Phi_w)\left.\frac{\partial Y}{\partial \Phi}\right|_w + \cdots. \quad (22b)$$

Since the cooled wall is along the horizontal axis in Fig. 1, $Y(\Psi, \Phi_w) = 0$. From the zeroth-order solution (when $h \to \infty$), $Y_0(\Psi, 1) = 0$. This yields the condition that $\partial Y_0/\partial \Psi|_\Phi = -\partial X_0/\partial \Phi|_\Psi = 0$ along the boundary $(\Psi, 1)$. For $h \to \infty (K \to 0)$ the $\Phi = 1$ along the cooled wall, so that for small K the Φ will be perturbed from unity and will generally vary slowly with Ψ along $\widehat{12}$. Hence in equation (20), $(\mathrm{d}\Phi/\mathrm{d}\Psi)^2 \ll 1$ and can be neglected; the accuracy of this approximation will be examined later by comparing numerical values of the solution at the wall to the exact boundary condition. Then equation (22b) becomes, after using $\partial Y/\partial \Phi|_w = \partial X/\partial \Psi|_w$,

$$KY_{\rm I}(\Psi, 1) = (1-\Phi_w)\left.\frac{\mathrm{d}X}{\mathrm{d}\Psi}\right|_w = -K. \quad (23)$$

This yields the boundary condition on the rectangle, $Y_{\rm I}(\Psi, 1) = -1$.

The boundary conditions for X and Y are summarized in Fig. 3.

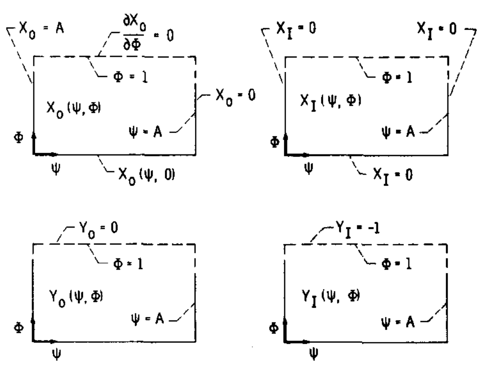

FIG. 3. Boundary conditions for components of $X(\Psi, \Phi)$ and $Y(\Psi, \Phi)$.

Solutions for $X_0, X_{\rm I}, Y_0, Y_{\rm I}$

The boundary conditions for X_0 are known on all sides of the rectangle as summarized in Fig. 3; the $X_0(\Psi, 0)$ satisfies equation (16). The solution, obtained by separation of variables, is

$$X_0(\Psi, \Phi) = A - \Psi + \sum_{n=1}^{\infty} C_n \sin\left(\frac{n\pi\Psi}{A}\right) \times \left\{\frac{\sinh(n\pi\Phi/A) + \sinh[n\pi(2-\Phi)/A]}{\sinh(2n\pi/A)}\right\} \quad (24)$$

where

$$C_n = \frac{2}{A}\int_0^A [X_0(\Psi, 0) - (A-\Psi)] \sin\left(\frac{n\pi\Psi}{A}\right) \mathrm{d}\Psi.$$

Then Y_0 is found as the conjugate harmonic function subject to the boundary condition in Fig. 3 to yield

$$Y_0(\Psi, \Phi) = 1 - \Phi + \sum_{n=1}^{\infty} C_n \cos\left(\frac{n\pi\Psi}{A}\right) \times \left\{\frac{\cosh(n\pi\Phi/A) - \cosh[n\pi(2-\Phi)/A]}{\sinh(2n\pi/A)}\right\}. \quad (25)$$

X_0 and Y_0 are the exact solution for the cooled wall at t_c ($h \to \infty$). The conjugate harmonic solutions that will satisfy the boundary conditions for $X_{\rm I}$ and $Y_{\rm I}$ shown in Fig. 3, are

$$X_{\rm I} = 0, \quad Y_{\rm I} = -1. \quad (26)$$

As discussed later, these simple forms show that, to a first level of approximation, the convective cooling produces a displacement of the interface without changing its shape.

Along the cooled wall $\widehat{12}$, the $Y = 0$. Then from equations (21b), (25) and (26), the variation of Φ_w with Ψ along the cooled wall can be found from

$$K = 1 - \Phi_w + \sum_{n=1}^{\infty} C_n \cos\left(\frac{n\pi\Psi}{A}\right) \times \left\{\frac{\cosh(n\pi\Phi_w/A) - \cosh[n\pi(2-\Phi_w)/A]}{\sinh(2n\pi/A)}\right\} \quad (27)$$

neglecting terms in K^2 and above.

Since approximations have been made in obtaining the perturbation solution, the accuracy in satisfying the boundary conditions should be checked. The condition in equation (11) is satisfied approximately, but all of the other boundary conditions are satisfied exactly. To check equation (11), a Cauchy–Riemann relation was used to obtain the form

$$-\left.\frac{\partial \Psi}{\partial X}\right|_w = \frac{1}{K}[1 - \Phi_w(X)]. \quad (28)$$

From equation (27) the $\Phi_w(\Psi)$ was found along the cooled wall and then $X_w(\Psi) = X(\Psi, \Phi_w)$ was found using equations (21a), (24) and (26). Equation (28) was then evaluated along the cooled wall. For the results in the next section the error in satisfying the boundary condition was usually less then about 1%. In a few extreme cases with large heating variations the error approached 4% along some small portions of the wall.

RESULTS AND DISCUSSION

The analytical results are in a general form with regard to the imposed heating distribution at the exposed phase-change interface. To illustrate the nature of the results, a heating variation is specified using a series expansion in Ψ,

$$Q(\Psi) = \left(1 - \sum_{n=1}^{\infty} E_n \cos\frac{n\pi\Psi}{A}\right)^{-1}. \tag{29}$$

To obtain $Q(X)$, the corresponding variation of X_s with Ψ is obtained by integrating equation (15)

$$X_s(\Psi) = X_0(\Psi, 0) = A - \Psi + \frac{A}{\pi}\sum_{n=1}^{\infty}\frac{1}{n}E_n \sin\left(\frac{n\pi\Psi}{A}\right). \tag{30}$$

By a trial-and-error adjustment of the E_n values, the $Q(X_s)$ variation can be approximately fitted to a desired incident heat flux variation. Another possibility is to insert the specified $Q(X_s)$ into equation (16) to obtain $\Psi(X_s)$ and hence $X_s(\Psi)$. The expression $X_s(\Psi) - A + \Psi$ is then expanded numerically in a Fourier sine series and compared with the series in equation (30) to obtain the E_n. From equations (24) and (30) the integral for C_n yields $C_n = (A/n\pi)E_n$. Then from equations (21) and (24)–(27),

$$\frac{X(\Psi, \Phi)}{A} = 1 - \frac{\Psi}{A} + \frac{1}{\pi}\sum_{n=1}^{\infty}\frac{1}{n}E_n \sin\left(\frac{n\pi\Psi}{A}\right) \times \left\{\frac{\sinh(n\pi\Phi/A) + \sinh[n\pi(2-\Phi)/A]}{\sinh(2n\pi/A)}\right\} \tag{31a}$$

$$\frac{Y(\Psi, \Phi)}{A} = \frac{1}{A} - \frac{\Phi}{A} + \frac{1}{\pi}\sum_{n=1}^{\infty}\frac{1}{n}E_n \cos\left(\frac{n\pi\Psi}{A}\right) \times \left\{\frac{\cosh(n\pi\Phi/A) - \cosh[n\pi(2-\Phi)/A]}{\sinh(2n\pi/A)}\right\} - \frac{K}{A} \tag{31b}$$

$$K = 1 - \Phi_w + \frac{A}{\pi}\sum_{n=1}^{\infty}\frac{1}{n}E_n \cos\left(\frac{n\pi\Psi}{A}\right) \times \left\{\frac{\cosh(n\pi\Phi_w/A) - \cosh[n\pi(2-\Phi_w)/A]}{\sinh(2n\pi/A)}\right\}. \tag{32}$$

To demonstrate the results in a simple yet informative way, the $Q(X)$ is obtained for a one-term series variation where the $E_n = 0$ for $n \geqslant 2$. The resulting $Q(X)$ distribution from equations (29) and (30) is shown in Fig. 4. For $E_1 = 0.4$ the heating varies with $x = 0$ to a by a factor of more than two, so the corresponding results for interface shapes will show the effect of appreciable variations in heat flux.

The interface shapes are readily calculated from equations (31a, b) by letting $\Phi = 0$. Results for $K = 0$ are shown in Fig. 5 for $E_1 = 0, 0.2, 0.4$ and $A = 1, 2, 4$. The $K = 0$ results are the exact solution for $h \to \infty$, for which the cooled wall is at uniform temperature t_c. The solid thickness is in inverse relation to the imposed heating. For small A the solidified region is thick and equations (31) (with $\Phi = 0$) show that the variation in shape about the mean thickness, $1/A$, approaches a limiting shape essentially equal to that for $A = 1$. For large A the solidified region is thin, and the shape approaches the configuration that would be predicted from a locally one-dimensional heat flow analysis. As a result, for $A = 4$, when $E_1 = 0.4$ the thickness changes by a factor of about two corresponding to a heating variation of about the same magnitude.

When K is nonzero ($h \neq \infty$) the solution shows that the thickness changes in a simple way according to equation (31b). The wall temperature is a variable along the cooled surface, and the analysis shows that, to the first level of approximation, the temperature variation does not affect the curvature along the free surface. The wall temperature variation is found as a function of Ψ from equation (32). If the $\Phi_w(\Psi)$ values are then used in

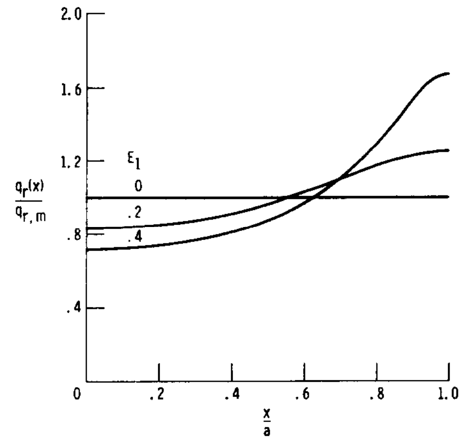

FIG. 4. Heating distributions along solidification interface.

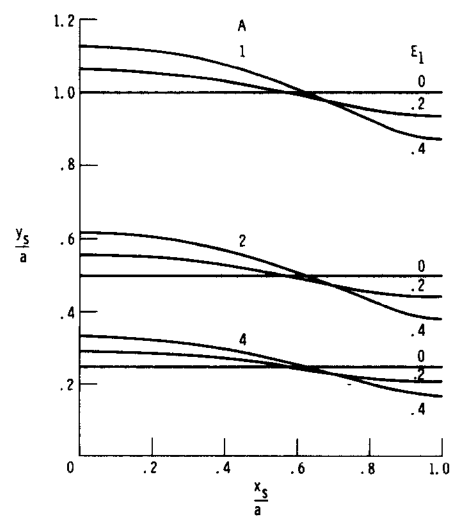

FIG. 5. Interface shapes when cooled boundary is at uniform temperature, $K = 0$.

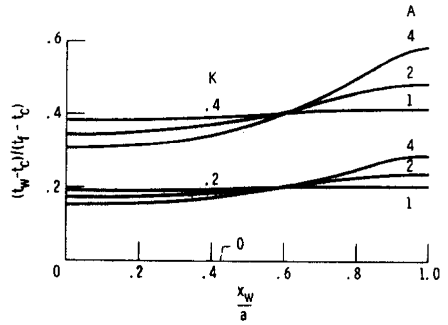

FIG. 6. Temperature distributions along convectively cooled wall.

equation (31a) the $X(\Psi, \Phi_w)$ is found, and the wall temperature variation plotted as in Fig. 6. This is of interest to numerically check the convective boundary condition which is approximated by the perturbation solution. As described in the analysis, the boundary condition was satisfied with good accuracy for all the illustrative results given here, including the most extreme cases where $E_1 = 0.4$ and $K = 0.4$.

CONCLUDING REMARKS

An analytical solution has been obtained for the response of a convectively cooled frozen layer to an imposed nonuniform radiative heating. For this type of heating, and with a high convective cooling heat transfer coefficient, an exact solution was obtained. This was accomplished by transforming the problem such that the physical coordinates were dependent variables of the temperature and a heat flow function; this transformed the solidified region into a rectangle in which an exact analytical solution can be found. When the convective cooling is not high, the transformed region deviates from being rectangular. A boundary perturbation was then used to transfer the boundary conditions to a fully rectangular region. The resulting approximate solution was found to satisfy the convective cooling boundary condition to within a very small error; the other boundary conditions, and the conduction equation in the region were satisfied exactly.

REFERENCES

1. J. R. Ockendon and W. R. Hodgkins (Editors), *Moving Boundary Problems in Heat Flow and Diffusion*. Clarendon Press, Oxford (1975).
2. R. Siegel and A. Snyder, Shape of porous region to control cooling along curved exit boundary, *Int. J. Heat Mass Transfer* **27**, 243–252 (1984).
3. R. H. Nilson and Y. G. Tsuei, Free boundary problem for the Laplace equation with application to ECM tool design, *J. appl. Mech.* **43**, 54–58 (1976).
4. G. Birkhoff and E. H. Zarantonello, *Jets, Wakes, and Cavities*. Academic Press, New York (1957).
5. G. E. Bell, An inverse solution for the steady temperature field within a solidified layer. *Int. J. Heat and Mass Transfer* **27**, 2331–2337 (1984).
6. R. Siegel, Conformal mapping for steady two-dimensional solidification on a cold surface in a flowing liquid, NASA TN D-4771 (1968).
7. E. Zauderer, *Partial Differential Equations of Applied Mathematics*. Wiley, New York (1983).
8. M. E. Goldstein and R. Siegel, Conformal mapping for heat conduction in a region with an unknown boundary, *Int. J. Heat and Mass Transfer* **13**, 1632–1636 (1970).

FORME DE LA FRONTIERE LIBRE D'UNE REGION CONGELEE PAR CONVECTION

Résumé—La forme bidimensionnelle d'une région solidifiée, telle que la couche gelée, est déterminée analytiquement pour la formation sur une plaque refroidie par convection. La forme non uniforme de la couche est produite par exposition à une distribution spatialement non uniforme d'énergie radiante. Pour un fort refroidissement par convection, la paroi refroidie approche une température uniforme et une solution exacte est obtenue pour la forme de la frontière libre. Pour un refroidissement moindre, la variation de température le long de la frontière refroidie est traitée par une méthode de perturbation. Quelques exemples sont traités pour montrer les effets du chauffage non uniforme et de l'importance du transfert thermique convectif à la paroi refroidie. Seule une condition limite est approchée par la solution de perturbation; toutes les autres conditions aux limites sont satisfaites exactement. Les résultats du calcul donnés ici satisfont la condition limite approchée avec une très faible erreur.

FORM DER FREIEN BEGRENZUNG EINES KONVEKTIV GEKÜHLTEN ERSTARRTEN GEBIETES

Zusammenfassung—Die zweidimensionale stationäre Form eines erstarrten Gebietes—einer Eisschicht z. B.—das einseitig von einer konvektiv gekühlten Platte begrenzt ist, wurde analytisch ermittelt. Die ungleichmäßige Form der Schicht wird durch eine räumlich ungleichmäßige Bestrahlung erreicht. Bei starker konvektiver Kühlung ergibt sich eine näherungsweise gleichmäßige Wandtemperatur, so daß man eine exakte Lösung für die Form der freien Begrenzung erhält. Bei geringerer konvektiver Kühlung wird der Temperaturverlauf entlang der gekühlten Begrenzung durch ein Strörungsverfahren behandelt. Einige anschauliche Beispiele zeigen die Einflüsse der ungleichförmigen Heizung und des konvektiven Wärmetransports an der gekühlten Wand. Nur eine Randbedingung wird durch das Störungsverfahren angenähert, alle anderen Randbedingungen werden exakt angesetzt. Die vorgestellten Rechenergebnisse weichen nur sehr wenig von den angenäherten Randbedingungen ab.

ФОРМА СВОБОДНОЙ ГРАНИЦЫ КОНВЕКТИВНО ОХЛАЖДАЕМОЙ ОБЛАСТИ ЗАТВЕРДЕВАНИЯ

Аннотация—Получено аналитическое выражение для формы двумерной установившейся области затвердевания, как, например, слоя инея, образующегося на конвективно охлаждаемой пластине. Неоднородность слоя вызвана пространственной неоднородностью распределения лучистой энергии, падающей на пластину. При чисто конвективном охлаждении температура стенки однородная. Получено точное решение для свободной границы. В том случае, когда конвективный перенос тепла составляет лишь часть полной энергии, изменение температуры вдоль границы исследуется методом возмущений. Приведены иллюстративные примеры, которые показывают влияние неоднородного нагрева на величину конвективного теплопереноса у охлаждаемой стенки. Только одно граничное условие аппроксимируется при решении методом возмущений, все остальные точно удовлетворены. Установлено, что результаты расчетов удовлетворяют приближенному граничному условию с очень небольшой погрешностью.